

Associated production of a Z boson and a b-jet in ATLAS

S. Diglio^{a,b}, A. Farilla^b, A. Tonazzo^{a,b}, M. Verducci^c.

^a *Dipartimento di Fisica, Universita' Roma Tre and INFN,*

^b *INFN Sezione di Roma Tre,*

^c *European Organization for Nuclear Research (CERN) and CNAF Bologna.*

Abstract

The current uncertainty on the parametrization of the partonic content of the proton (PDF's) affects the potential for the discovery of new physics at LHC. The study of Z boson production in association with a b-jet can considerably reduce such uncertainty. In addition, this process represents a background both to the search for the Higgs boson and for SUSY particles. We present an update, based on the full simulation data sample produced for the Rome Physics Workshop, of a preliminary study [1] in the case where the Z boson decays in $\mu^+\mu^-$.

1 Introduction

The production of electroweak gauge bosons (W^\pm, Z, γ) together with jets containing heavy-quarks (c, b) is an important signal at the hadron colliders. The simplest process involves a boson and one heavy-quark jet. In this work, the production of Z boson will be taken into account, $gQ \rightarrow ZQ$ (where Q is a b or c quark). The cross sections at the next-leading-order, see [2], will be used to estimate the number of expected events and finally a comparison with the Tevatron experiment will be done.

The Feynman diagram of the production of a Z boson and a heavy-quark jet via $gQ \rightarrow ZQ$, shown in figure 1, can probe the parton distribution function (PDF) of the b quark, because the initial state involves a b quark from the sea. In addition, this channel is very important because it is a possible background for $gb \rightarrow hb$, where the Z boson and the Higgs boson decay to the same final state ($b\bar{b}, \tau^+\tau^-, \mu^+\mu^-$), see figure 2 [3].

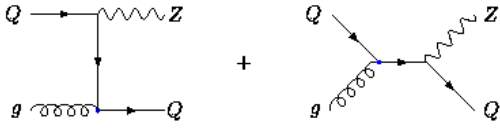


Figure 1: Associated production of a Z boson and a single high- p_T heavy quark ($Q=c,b$).

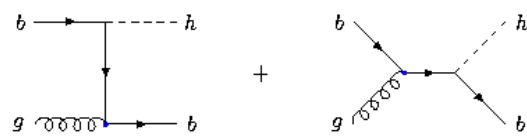


Figure 2: Associated production of the Higgs boson and a single high- p_T bottom quark.

The Z boson with a heavy-quark jet is a possible background for SUSY events characterized by multiple jets, leptons, and missing transverse energy E_T^{miss} . Looking at the plot of the “effective mass” shown in figure 3, defined as the scalar sum of the missing energy and the transverse momenta of the hardest jets, the Z+jets channels represents one of most significant Standard Model background.

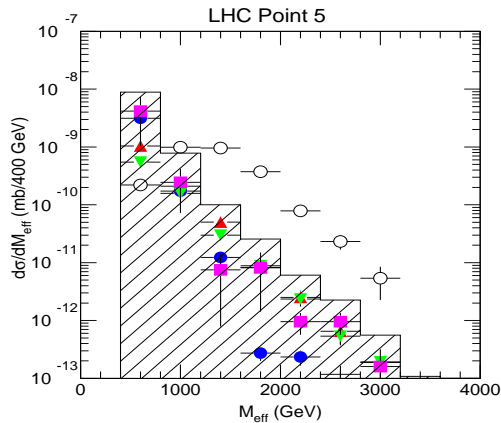


Figure 3: M_{eff} distribution for the signal (open circles) and for the sum of all Standard Model backgrounds (histogram); the latter includes $t\bar{t}$ (solid circles), W +jets (triangles), Z +jets (downward triangles), and QCD jets (squares), [4].

Z+jet events will be used to calibrate the calorimetric jet energy measurements, profiting from the high statistics and a relative low and well known background.

Performing an “in situ calibration”, it will be possible to calibrate the calorimeters using jets reconstructed in the experiment. This aspect will not be included in this note, for more details see [5] and [6].

2 Study of the Parton Distribution Function (PDF)

At the LHC, every measurement will be deeply affected by the uncertainties related to the knowledge of PDFs, since the production cross section in a proton-proton collision is given by the convolution of the partonic cross sections with the PDFs.

Since the kinematic space accessible at the LHC will be much broader than at previous experiments, it will be possible to study the PDFs both at the Electroweak mass scale (W and Z Mass), where the low x-gluon contribution will be more significant, and at the TeV scale where the high x-gluon will be the dominant contribution.

Figure 4 shows the kinematic region in the plane (x, Q^2) at different values of η and mass scale for different experiments. It is important to underline that the plane for LHC will be greater than at previous experiments and that there will be some regions accessible both by LHC and the experiments at HERA representing a good cross check for the first measurements at LHC.

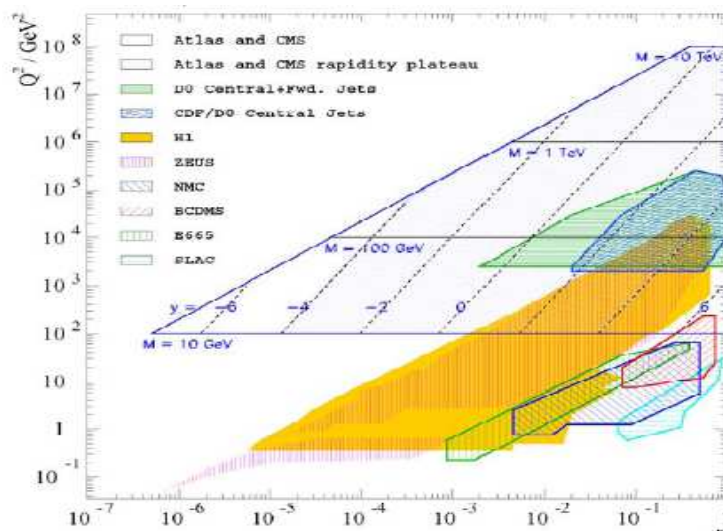


Figure 4: LHC kinematical plane in comparison with other experiments.

In this paper we will focus on the possibility to study the b-PDF using the Z boson production in association with a jet.

The knowledge of the b PDF is directly related to the uncertainties on the Z production cross section. At LHC, the contribution to the total Z production from $b\bar{b} \rightarrow Z$ will be about 5%, see plot in figure 6, consequently a precision of $\approx 1\%$ in the measurement of the Z boson cross section will imply a precision of the b PDF of at least $\approx 20\%$. The results obtained by HERA are now far from this level of accuracy, see [7].

The sensitivity to the b PDF is enhanced in processes such as those shown in figure 1, involving the

production of a Z boson in association with a b quark. At LHC we expect to have a very large statistics of such events, providing a measurement that will mainly depend on systematic uncertainties. Some preliminary studies on the p_T distributions for the jets for different sets of events generated with different PDFs have shown that we could have differences in the low p_T region of the order of $\approx 5\%$, see plots in figure 5 for the η and p_T distributions. The measurement will be sensitive if the systematic uncertainties can be kept below this level.

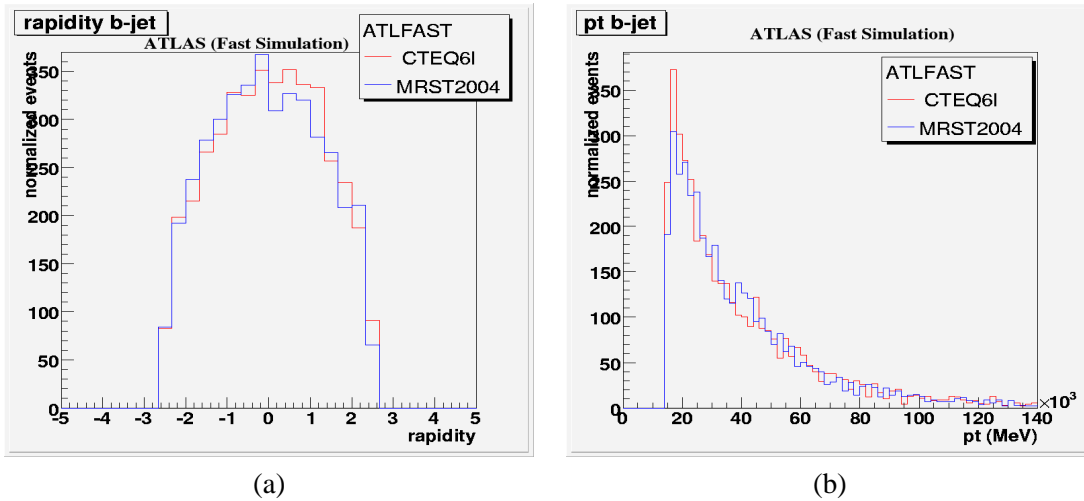


Figure 5: (a) η distribution of the b -jets in Zb events (ATLFast) (b) p_T distribution of the b -jets in Zb events (ATLFast).

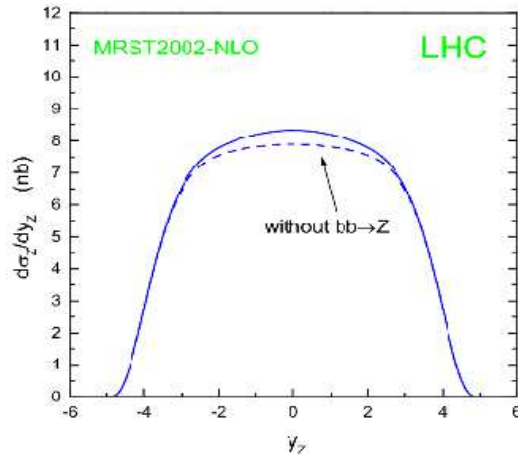


Figure 6: Contribution of the $b\bar{b} \rightarrow Z$ to the total Z production at LHC as function of the rapidity, see [7].

As said before, the main leading order contribution will be due to the $gQ \rightarrow ZQ$ channel. The possible sources for ZQ production, see table 1, are:

- $gQ \rightarrow ZQ$
calculated at the leading order and at the next-to-leading order via the subprocesses:
 - $gQ \rightarrow ZQ$,
 - $qQ \rightarrow ZqQ$,
 - $gQ \rightarrow ZgQ$,
 - $gg \rightarrow ZQ\bar{Q}$,
- $q\bar{q} \rightarrow ZQ\bar{Q}$
calculated only at the leading order with one Q out of detector acceptance. Figure 7 shows the Feynman diagrams, where one of the Q quark is missed or two Q quarks are together in a single jet. Nevertheless, this process is more significant at Tevatron than at LHC.
- $q\bar{q} \rightarrow Zg, gq \rightarrow Zq$
calculated at the leading and next-to-leading order for events Z+j or Z+jj.
- $gg \rightarrow ZQ\bar{Q}$
this process allow the emission of one Q collinear to the beam yielding to ZQ in the final state. This approach, with m_Q non equal to zero, however, has some problems with the calculations, in fact the perturbation theory results less convergent ($\alpha_S \ln(M_Z/m_Q)$ instead of α_S) and it is much more difficult to obtain the next-to-leading order correction. This case is not included in this study.

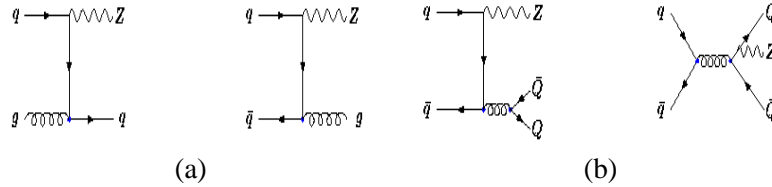


Figure 7: (a) Feynman diagrams for Zj production via $gq \rightarrow Zq$ and $q\bar{q} \rightarrow Zg$, where q are light quarks. (b) Feynman diagrams for $q\bar{q} \rightarrow ZQ\bar{Q}$.

Table 1 gives the cross sections of the processes described above at the leading and next-to-leading order, from the study [2]. We defined the process Zb as signal and the other processes as possible backgrounds.

The motivations to study this process at LHC appear more evident from the comparison with the Tevatron cross sections. First of all, we notice that the total cross section for Z+b production is about 1090 pb at LHC, a factor of about 50 larger than at the Tevatron. We also remark that the contribution to Z+b production from $gb \rightarrow Zb$, which is the most important for the sensitivity to the b PDF, is much more significant at the LHC. Finally, at the LHC, the relative importance of processes other than Z+b (such as Zc, Zq and Zg) is less relevant than at the Tevatron; in addition, the probability of mis-tagging a light jet as a heavy quark is smaller, therefore the LHC provides a cleaner environment for the extraction of the Z+b signal. And the total cross section for Zc production is more important at Tevatron (about 70% greater than Zb) than at LHC (about 35% greater than Zb).

Cross Section(pb)	Tevatron	LHC
Process	ZQ inclusive	
$gb \rightarrow Zb$	$13.4 \pm 0.9 \pm 0.8 \pm 0.8$	$1040^{+70+70+30}_{-60-100-50}$
$q\bar{q} \rightarrow Zb\bar{b}$	6.83	49.2
$gc \rightarrow Zc$	$20.3^{+1.8}_{-1.5} \pm 0.1^{+1.3}_{-1.2}$	$1390 \pm 100^{+60+40}_{-70-80}$
$q\bar{q} \rightarrow Zc\bar{c}$	13.8	89.7
	Zj inclusive	
$gq \rightarrow Zq, q\bar{q} \rightarrow Zg$	$1010^{+44+9+7}_{-40-2-12}$	$15870^{+900+60+300}_{-600-300-500}$

Table 1: Next-to-leading-order inclusive cross section (pb) for Z Boson production in association with heavy-quark jets at the LHC ($\sqrt{s} = 14TeVpp$) and Tevatron ($\sqrt{s} = 1.96TeVpp$). The calculations are limited to the case of a jet in a range $p_T > 15GeV$ and $|\eta| < 2.5$ (LHC) or $|\eta| < 2.0$ (Tevatron). The labels on the columns mean: ZQ = Z plus one jet, which contains a heavy quark, while Zj = Z plus one light jet, which does not contain a heavy quark, [2]. The process Zb represents the signal of this study while all the other processes some possible backgrounds.

Finally, due to a relatively smaller contribution of $q\bar{q} \rightarrow ZQ\bar{Q}$ and, for Zj events, a smaller probability of mis-tagging a light jet as a heavy quark, LHC provides a clearer environment for the extraction of the Zb signal.

D0 [8] has provided some measurements of the cross section ratio: (Z+bjet)/(Z+jet) within a kinematical region similar to the one in this note. The result is in agreement with the same ratio obtained in CDF, [9], and with the NLO calculations reported in [2].

In the following calculations, the values of the cross sections, shown in table 1, will be used.

3 Simulated Data Sample

All the samples used have been generated using the PYTHIA MonteCarlo package [10] and [11]. The contribution from virtual photon production (Drell-Yan) was switched off, and only the decays of the Z boson to muons were enabled.

The simulation of the data has been performed using, for the detector description, the Rome Layout, defined for the Atlas Physics Workshop held on June 2005 in Rome.

In detail we used:

- $Z + jet$ with $Z \rightarrow \mu\mu$ about 500k events (*umich.004290.reco1004.ZJET010020_mumu*)
- $W + jet$ with $W \rightarrow lepton + \nu$ about 300k events
(*umich.004285.reco1004.WJET010020_lepnu* for the systematics studies)

Only the decays $W \rightarrow \mu\nu$ and $Z \rightarrow \mu\mu$ have been considered. The W +jet process, with $W \rightarrow \mu\nu$, has been used to estimate the systematics errors due to the mis-tagging.

The events have been analyzed using the combined Ntuples produced by RecExCommon, the official Atlas software reconstruction package inside ATHENA. In this package there are dedicated

algorithms for the reconstruction of different trigger-objects like jets, leptons, photons or B-tagging algorithms to identify jet flavor. In particular, for the B-tagging we used the Cone algorithm, explained in detail in section 9. While for the muon identification, there are two packages: MOORE and MUID, that perform the muon reconstruction in the Muon Spectrometer, including the corrections due to the multiple scattering and the energy loss in the inert material as described in detail in [12], [13] and [14].

4 Event Selection Criteria

The selection reported in this work, defined a strategy to select, in the first place, events with Z and one jet, then to identify in these events a Z boson associated with a jet from a b quark. Two different and independent b-jet identification algorithms have been used: “the inclusive b-tagging” and “the soft muon tagging”, described below.

The signal was defined as the events containing a Z boson decaying into a couple of muons and a b jet with a $p_T \geq 15\text{GeV}$ and $|\eta| \leq 2.5$. The background samples containing respectively a c-jet within the same cuts, or a jet originating from a light quark or a gluon in the same range, were considered separately. The NLO cross-sections computed in table 1 were used for the signal and for these two classes of background, while the cross-section given by PYTHIA was taken for the events with a jet from light quark or gluon.

In the section below the selection performances of Z+jet events with the two b-tagging algorithms are presented.

The quality of the event selection has been estimated using the ratio variables: *efficiency* and *purity*. The efficiency is defined as the ratio between the number of selected signal events over the total number of events while the purity is given by the ratio between the number of events with a b-quark and the number of selected signal events.

The number of expected events is estimated using the formulas (1), where we used the cross sections at the NLO, taking into account the different efficiencies of selection: ϵ_{acc} due to the geometric acceptance, ϵ_{cuts} for the cuts applied for the di-muon invariant mass and finally ϵ_x for the selection of the sample with the jet of a particular flavor.

$$\begin{aligned}
 N_b &= \sigma_b^{table} \cdot BR(Z \rightarrow \mu\mu) \cdot \mathcal{L} \cdot \delta t \cdot \epsilon_{acc} \cdot \epsilon_{cuts} \cdot \epsilon_b \\
 N_c &= \sigma_c^{table} \cdot BR(Z \rightarrow \mu\mu) \cdot \mathcal{L} \cdot \delta t \cdot \epsilon_{acc} \cdot \epsilon_{cuts} \cdot \epsilon_c \\
 N_{oth} &= \sigma_{other}^{Pythia} \cdot BR(Z \rightarrow \mu\mu) \cdot \mathcal{L} \cdot \delta t \cdot \epsilon_{acc} \cdot \epsilon_{cuts} \cdot \epsilon_{oth}
 \end{aligned}
 \tag{1}$$

An estimation of the number of events expected for 30fb^{-1} of integrated luminosity has been provided.

4.1 Z+jet Events

The selection of these events will be primarily affected by the trigger efficiency. The trigger efficiency (2mu20 trigger menu) is high and about 95% [16], thanks to the presence of one or more high P_T muons in the event. This is the major advantage of this channel with respect to the other events with b quarks.

Concerning the efficiency of the muon reconstruction algorithm, MUID, has a selection efficiency in the p_T range of the muons from Z boson decay of more than 95% for $|\eta| < 2.5$.

The sample of Z +jet events was selected requiring two high p_T muons satisfying the following kinematic cuts, and at least one jet:

- two muons of opposite charge,
- both muons with $p_T \geq 20$ GeV,
- di-muon invariant mass in the range $70 \leq M^{\mu\mu} \leq 110$ GeV,
- and one jet.

In the case where there are more than two muons satisfying the cuts all the possible combinations for di-muon invariant mass have been taken into account, the best one has been chosen.

To define the geometric acceptance of the detector and the coverage of reconstruction software, these additional cuts have been required:

- two muons in $|\eta| \leq 2.5$,
- one jet in $|\eta| \leq 2.5$ and $p_T > 15$ GeV.

Figure 8 shows the di-muon invariant mass plots obtained by MonteCarlo Truth (a) and by MUID (b) respectively after these cuts.

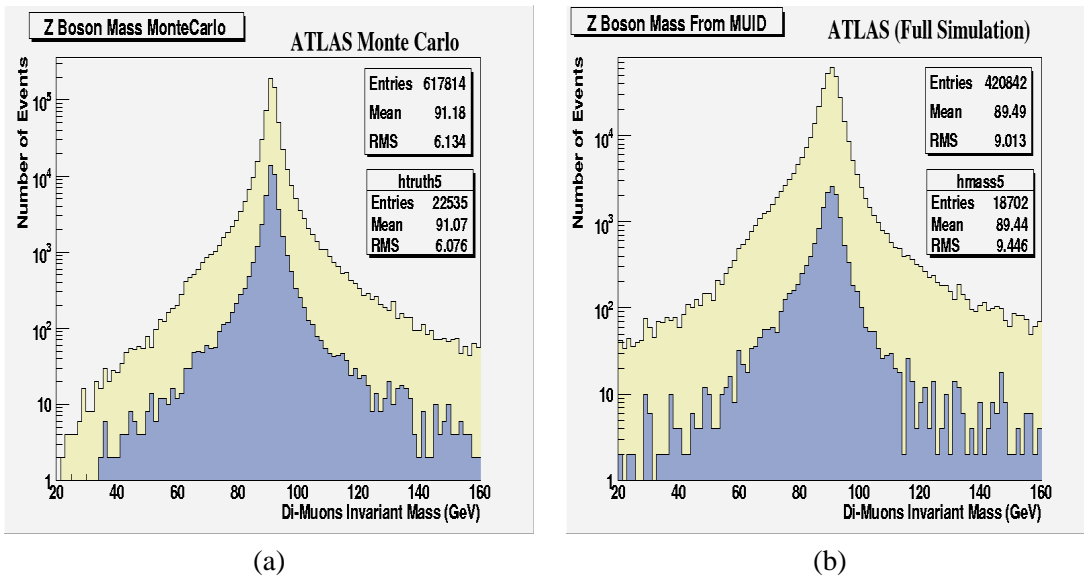


Figure 8: (a) Di-muon invariant mass from MonteCarlo information, (b) same plot but obtained with the reconstruction package MUID. The same cuts are applied in the plots, requiring two muons with $|\eta| < 2.5$ and with a $p_T > 20$ GeV. The dark (blue) histogram represents the events with b -quark.

4.2 Z+b-jet Events

4.2.1 Secondary Vertex b-Tagging

The inclusive b-tagging algorithm is used to identify the jet of b flavor, see [15] for additional information about the algorithm.

The jet is identified with the Cone algorithm with $\Delta R = \sqrt{(\Delta\phi)^2 + (\Delta\eta)^2} = 0.7$, and requiring:

- at least one track selected in the tracker for jet tagging,
- cut on the b-tagging weight $w_t > 3$. Tracks from B-hadrons decays are expected to have on average a large and positive transverse impact parameter a_0 and a large and positive longitudinal impact parameter z_0 , but less discriminating. Combining the longitudinal and transverse significance in the function: $w_t = P_b(S_{a_0, z_0})/P_u(S_{a_0, z_0})$ and applying the previous cut on the likelihood function is possible to discriminate b-jet from light jets.

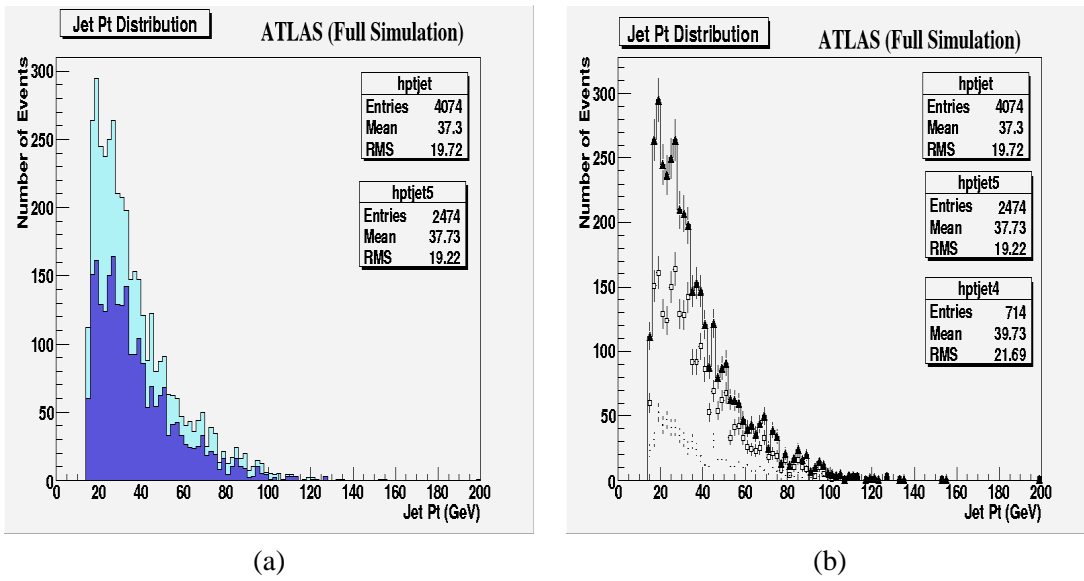


Figure 9: (a) P_T distribution of jets obtained after the cuts on the di-muon invariant mass and the b-tagging jet selection. The dark area represents the tagged b-jets. (b) P_T spectrum of jets obtained after the cuts on the di-muon invariant mass and the jet. The b (squares - hptjet5) and c (dotted line - hptjet4) jets are shown separately with respect the total jets sample (line and black triangle - hptjet).

The obtained purity and the expected number of events are reported in table 2. Figures 9 show the P_T spectrum of jets in the selected events, while the figures 10 the distributions of the eta and phi variables for the jets selected by the b-tagging algorithm. The fact that b-tagged jets tend to have a higher P_T implies that the efficiency and purity of the selected sample improve after the additional cut of the $p_T > 15\text{GeV}$. The relative quantity of b-jets with respect of the total number of selected jets is about 60% while the contamination from c-jets is about 20% in all the P_T range, as shown in detail in the table 3 .

B-TAGGING	
CUTS	Efficiency
μ in $ \eta < 2.5$	49.9%
$p_T > 20\text{GeV}$ and $70 < \text{Mass} < 110\text{GeV}$	59.5%
B-tagging Algo	56.2%
Purity	60.7%
Number of b Events	176642
Number of Background Events	204265

Table 2: The efficiencies, the purity and the number of estimated events with the full simulation for the b-tagging algorithm. The number of events is calculated for 30 fb^{-1} of integrated luminosity. The b,c jets selected satisfied the cuts on p_T and η : $p_T > 15\text{GeV}$ and $|\eta| \leq 2.5$

B-TAGGING		
P_T Range in GeV	b jets %	c jets %
15-25	54.2	17.2
25-35	63.2	15.4
35-45	75.6	14.6
45-55	58.2	20.3
55-65	58.7	21.4
65-75	59.8	21.1
75-200	47.8	24.7

Table 3: Population of b-jets and c-jets, divided in P_T range, after the B-Tagging selection and the additional cuts on the jets of η : $p_T > 15\text{GeV}$ and $|\eta| \leq 2.5$

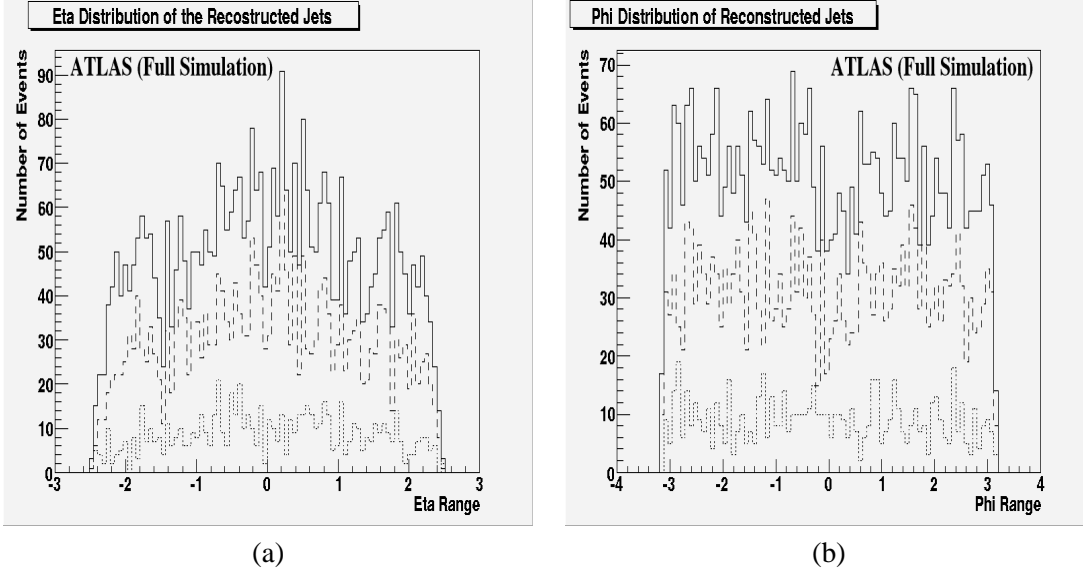


Figure 10: (a) *Eta* distribution of jets obtained after the cuts on the di-muon invariant mass and the *b*-tagging jet selection. The *b* (dash line) and *c* (dotted line) jets are shown separately with respect the total jets sample (full line). (b) *Phi* distribution of jets obtained after the cuts on the di-muon invariant mass and the *b*-tagging jet selection, shown with the same labels.

A first estimation of the ratio between the Z+bjet cross section over the total production cross section of Z+jet is given, taking into account the results obtained for the 30 fb^{-1} of integrated luminosity and only for the inclusive B-Tagging selection.

The cross section ratio is defined as the ratio of the number of events obtained after the b-tagging selection over the total number of Z+jet events multiplied for the ratio of the selection efficiencies and the ratio of the purities of the samples. In detail:

$$Ratio = \frac{\sigma_{Z+bjet}}{\sigma_{Z+jet}} = \frac{N_b}{N_{tot}} \cdot \frac{\epsilon_{1jet}}{\epsilon_{1bjet}} \cdot \frac{f_{B \rightarrow b}}{1} = \frac{4074}{114881} \cdot \frac{0.6}{0.6} = 0.035 \quad (2)$$

where $\epsilon_{onejet}/\epsilon_{onebjet} = 1/\epsilon_{BTag} \approx 0.6$, see [15], $f_{B \rightarrow b} = 1 - f_{C \rightarrow b} - f_{lightquark \rightarrow b} \approx 0.6$. The statistical error $\sigma(stat)$ is less than 10^{-4} due to the high statistics and the systematic error $\sigma(syst)$ is still under evaluation, it is expected to be $\leq 10\%$. The value of the ratio obtained by the D0 measurement for 180 pb^{-1} , is: $R = 0.019 \pm 0.005(stat)$ [8].

SOFT MUON TAGGING	
CUTS	Efficiency
μ in $ \eta < 2.5$	49.9%
$p_T > 20\text{GeV}$ and $70 < \text{Mass} < 110\text{GeV}$	59.5%
Third Muon Algo	7.2%
Purity	37.2%
Number of b Events	22630
Number of Background Events	68088

Table 4: The Efficiencies, the purity and the number of events estimated with the full simulation for the soft muon tagging algorithm. The b,c jets selected satisfied the cuts on p_T and η : $p_T > 15\text{GeV}$ and $|\eta| \leq 2.5$. The number of expected events are calculated for an integrated luminosity of 30 fb^{-1} .

4.2.2 Soft Muon Tagging

The soft muon tagging provides an independent way from the usual b-tagging algorithm to identify the b-jet using the muon from the semileptonic decay of a b-meson.

At this stage, we have only looked for a third muon in the Muon Spectrometer that has been reconstructed by MUID. Typically, the muon inside the b-jet can reach the middle station of the Muon Spectrometer to be reconstructed. The efficiency of this selection is intrinsically low, depending on the few muons that can reach the Spectrometer after have lost 2-3 GeV in the calorimeters, but the purity obtained is rather good, introducing a cut on the transverse momentum of the muon the purity increases. The simple request of a third muon in the soft muon-tagging implies an underestimation of the relative background.

In the table 4 the purity and the number of expected events for 30 fb^{-1} of integrated luminosity are given.

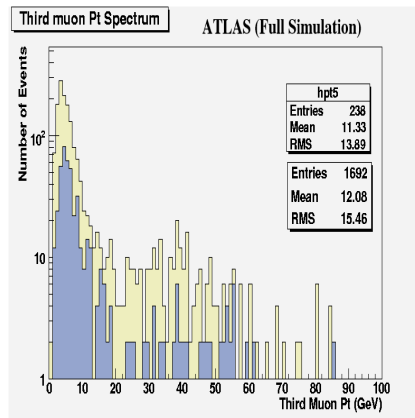


Figure 11: Third muon P_T distribution obtained after all cuts and requiring at least one jet. The muon P_T is reconstructed in the Muon Spectrometer using the MUID reconstruction algorithm.

4.2.3 Further Studies on the b Jets Discriminants

The major source of background in our selected events is represented by c-jets tagged as b-jets.

We have studied which variables can be used to better discriminate the signal events with respect to the background events after the b-tagging algorithms (inclusive b-tagging and soft muon tagging) have been applied.

Taking into account the results of ZEUS, H1 and CDF, we have investigated, as possible discriminating variable, the muon transverse momentum relative to the axis of associated jet.

The relative momentum is given by:

$$p_T^{Rel} = |\vec{p}_\mu| \sin(\arccos(\frac{\vec{p}_\mu \cdot \vec{p}_{jet}}{|\vec{p}_\mu| |\vec{p}_{jet}|})) \quad (3)$$

The b events show to have a p_T^{Rel} values greater than the c events, as it is shown in the plots in figure 12 due to the bigger mass of the b quark. Further variables will be studied to have a good discriminator between signal and background for the selected events.

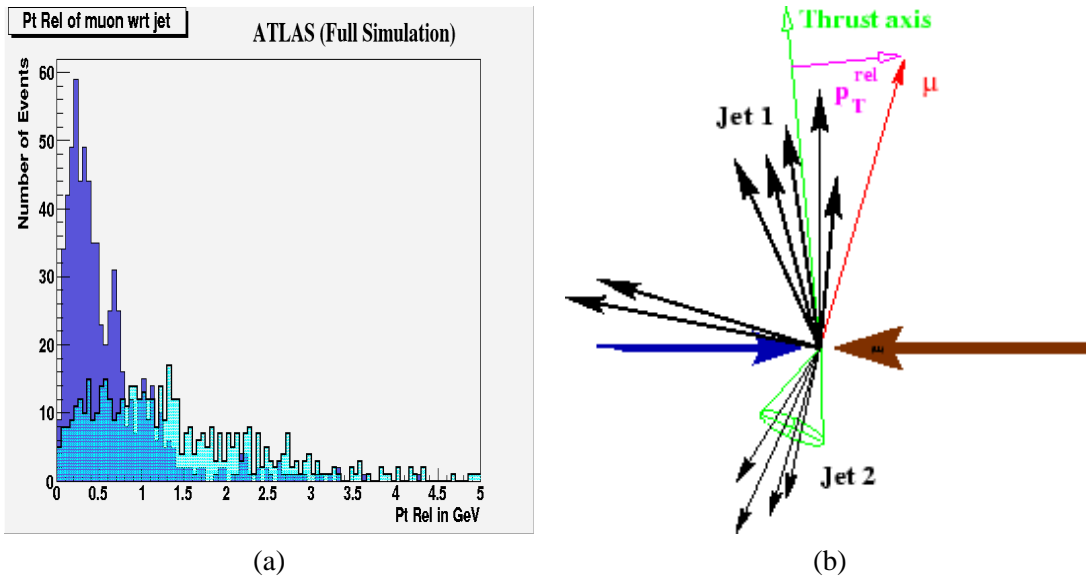


Figure 12: (a) The p_T^{Rel} distributions for charm (dark plot, less spread, with the maximum less than 1 GeV) and beauty (more spread and flat) events. This plots have been obtained using the MonteCarlo information for the jets and the muons. (b) Draft of the p_T^{Rel} .

5 Systematic effects on the selection

Given the large statistics of the available data samples, the measurement will be limited by systematic effects which will be mainly due to the knowledge of the selection efficiency and background estimation.

We have investigated the possibility to control these effects directly from data sample itself. The b-tagging efficiency can be checked using b -enriched samples. Based on previous experience at

Tevatron and LEP, we can expect a relative uncertainty of about 5%.

The background in the selected sample is mainly due to mis-tagged jets from c and light quarks. This can be controlled by looking at the number of tagged jets in data samples that in principle should not contain b -jets at first order: W +jets, for example, are such a kind of events.

The W +jet events will be available with large statistics, moreover jets produced in association with W boson will cover the full p_T range of the signal.

On this bases we decided to use a W +jets sample (generated using PYTHIA [10] and processed with a complete simulation of ATLAS detector, based on GEANT4 [19]) to estimate systematic uncertainties on b -tagging.

We analyzed only events containing a muon from W decay within the following kinematic cuts (that are the same cuts used to select muons from Z decay in the Z +jet sample):

- at least one muon in the event with:
 - $p_T > 20$ GeV;
 - $|\eta| < 2.5$;
- at least one reconstructed jet.

After this selection on muons, we looked for events where at least one jet is tagged as a b -jet. In this way it has been possible to calculate the number of mis-tagged jet with respect to the total number of jets as function of the jet p_T .

As we can see in figure 13 we expect to estimate the background from mis-tagging with a relative uncertainty at the level of few percent over the full p_T range of the signal.

This result is in good agreement with previous results obtained using fast simulation on a W +jet sample [17].

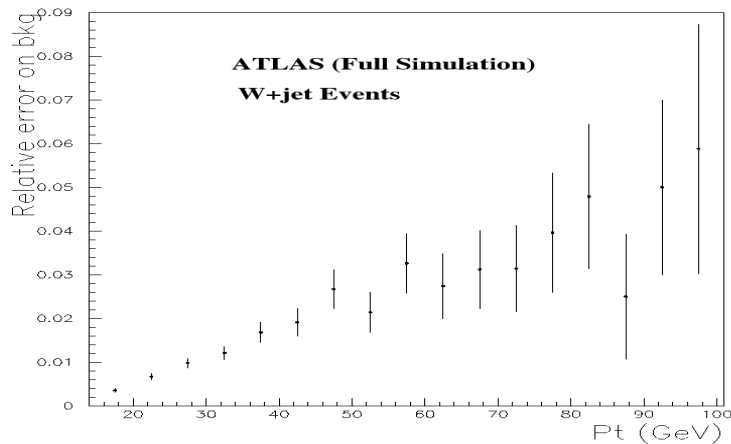


Figure 13: Systematics due to mis-tagging of b -jets evaluated from fraction of b -tagging jets in the W +jets sample: relative error on background level per 5 GeV jet p_T bin.

The systematics due to the calibrations of the detectors, according to the same studies [5, 6] will be of the order of few percent, this value is under investigation and will be checked using the data

simulated for the Computing System Commissioning CSC-06. Further studies are in progress to define the energy scale and resolution of the reconstructed jets.

6 Conclusions and outlook

In the LHC physics program, the Z+jet analysis has an important role, it represents a clear and high statistics channel to perform studies on the PDFs in particular on the b-PDF, and consequently to improve the precision of the other production cross sections of topics signatures as Higgs or SUSY. The high statistics expected after all the analysis chain will provide a sample of a relevant purity with a small statistical error. The measurement will be affected principally by the systematic uncertainties.

Further studies will follow on the analysis of the data samples simulated with the underlying and minimum bias events at low luminosity.

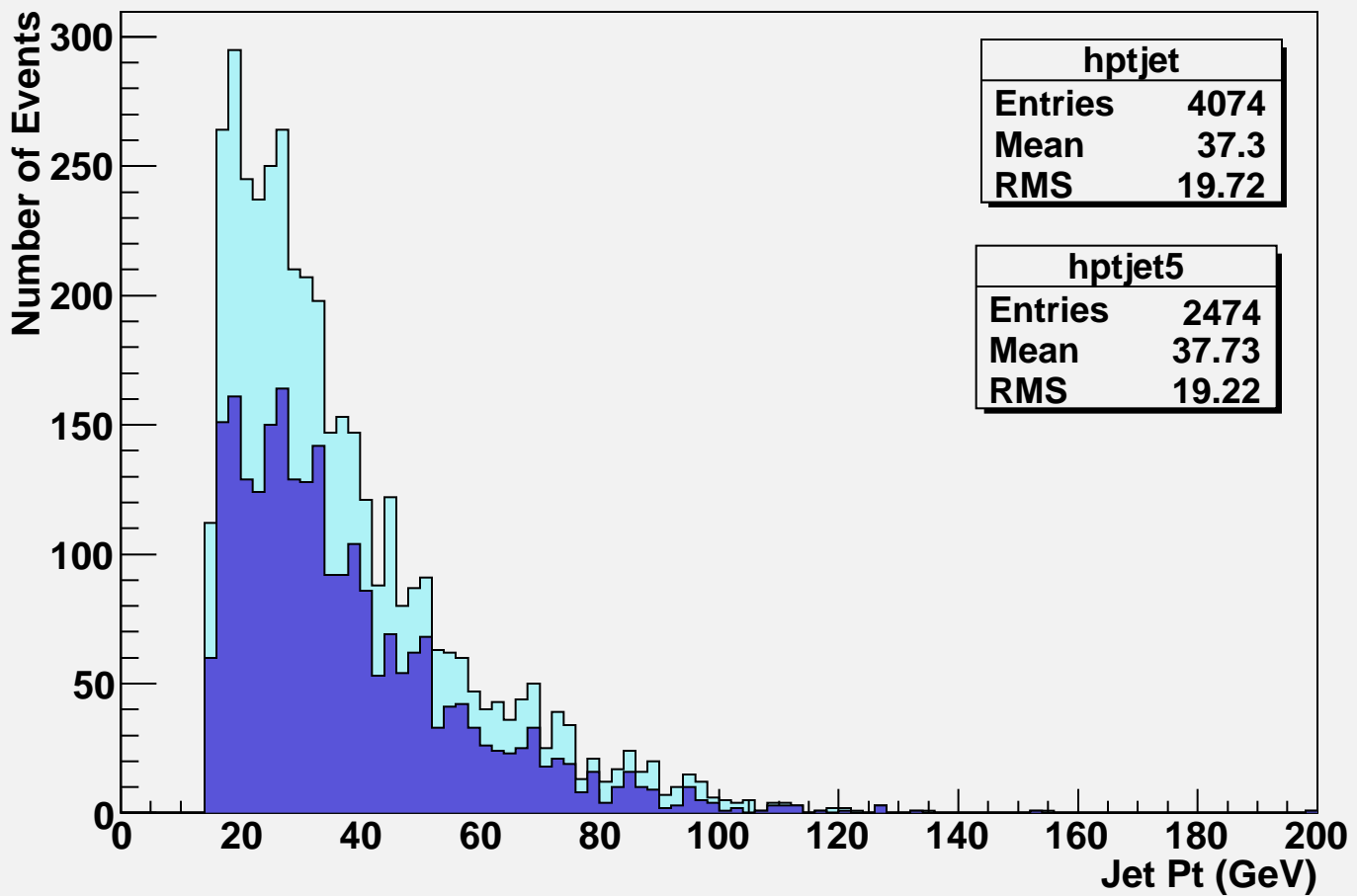
A more complete analysis concerning systematic effects and the impact of the varies sets of pdf is already being done with the CSC data.

References

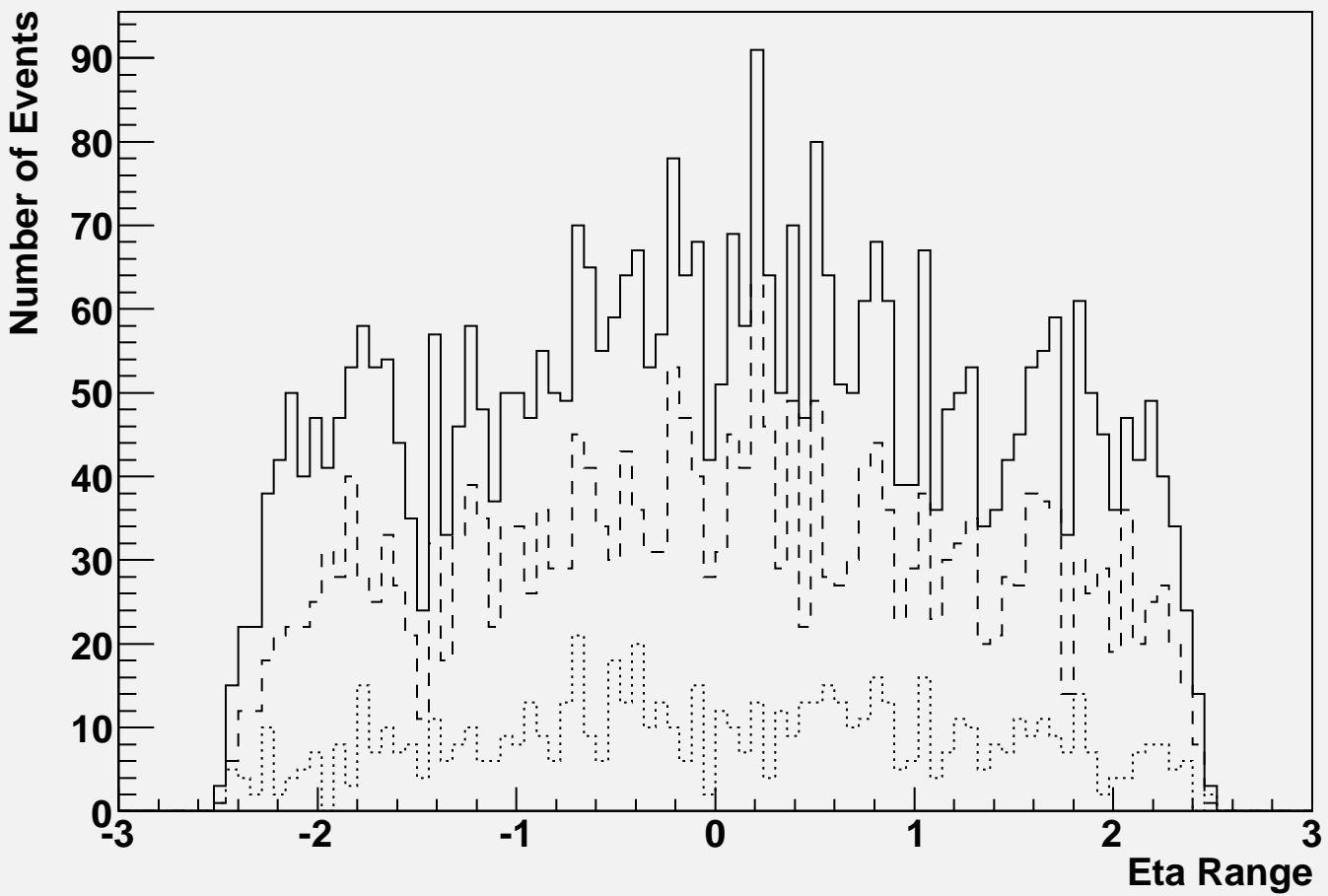
- [1] S.Diglio, A.Tonazzo, M.Verducci, *A preliminary study of Z+b production at LHC*, ATL-COM-PHYS-2004-078, 2004
- [2] J.Campbell, R.K.Ellis, F.Maltoni and S.Willenbrock, *Associated production of a Z Boson and a single heavy quark jet*, Phys.Rev.D69:074021, 2004
- [3] J.Campbell, R.K.Ellis, F.Maltoni, S.Willenbrock, *Higgs-Boson production in association with a single bottom quark* Phys.Rev.D67:095002, 2003
- [4] ATLAS Collaboration *ATLAS Detector and Physics Performance Technical Design Report*, CERN/LHCC/1999-15, (1999)
- [5] R.Lefevre, C.Santoni *In situ determination of the scale and resolution of the jet energy measurements using $Z^0 + jets$ events*, ATLAS Internal Note, ATL-PHYS-2002-026, 2002
- [6] J. Proudfoot, et al. *Jet Energy Scale Calibration in Vector Boson Events using Rome Simulation Data*, ATLAS Internal Note, ATL-COM-PHYS-2005-067, 2005
- [7] S.Alekhin, et al. *HERA and LHC, a Workshop on the implications of HERA for LHC physics*, CERN-2005-014, DESY-PROC-2005-001
- [8] DO Note 4388, The DO Collaboration, Phys. Rev. Lett. **94** 161801 (2005);
- [9] CDF Collaboration, *Measurement of the b Jet Cross Section in Events with a Z Boson in $p\bar{p}$ Collisions at $\sqrt{s} = 1.96\text{TeV}$* , hep-ex/0605099, May 2006
- [10] T. Sjöstrand, P. Eden, C. Friberg, L. Lönnblad, G.Miu, S.Mrenna, E.Norrbin, *PYTHIA 6.2 Physics and Manual*, Computer Physics Commun 135, (2001) 238
- [11] Atlas Collaboration Manual,
http://wwwinfo.cern.ch/asdoc/psdir/pythiarus/pythia_rus.ps.gz
- [12] D.Adams, et al., Atlas Internal Note, ATL-SOFT-2003-008, ATL-DAQ-2003-02, 2003
- [13] D.Adams, et al., ATLAS Internal Note, ATL-SOFT-2003-007, 2003
- [14] D.Adams, et al., ATLAS Internal Note, ATL-CONF-2003-011, 2003
- [15] S. Correard et al. *b-tagging with DC1 data*, ATL-PHYS-2004-006, (2004)
- [16] ATLAS Collaboration *ATLAS High-Level Triggers, DAQ and DCS Technical Proposal*, CERN/LHCC/2000-17, (2000)
- [17] M. Cacciari, E. Laenen, S. Diglio, A. Tonazzo, M. Verducci et. al. *Theoretical review of various approaches in heavy quark production*, CERN-2005-014 (14 December 2005)[arXiv:hep-ph/0601012-3]
- [18] A. Cooper-Sarkar, M. Dittmar, D.C. Gwenlan, H. Stenzel, A. Tricoli *LHC final states and their potential experimental and theoretical accuracies*, CERN-2005-014 (14 December 2005)

- [19] S. Agostinelli et al., *Geant4 - A Simulation Toolkit*, Nuclear Instruments and Methods A 506 (2003) 250-303

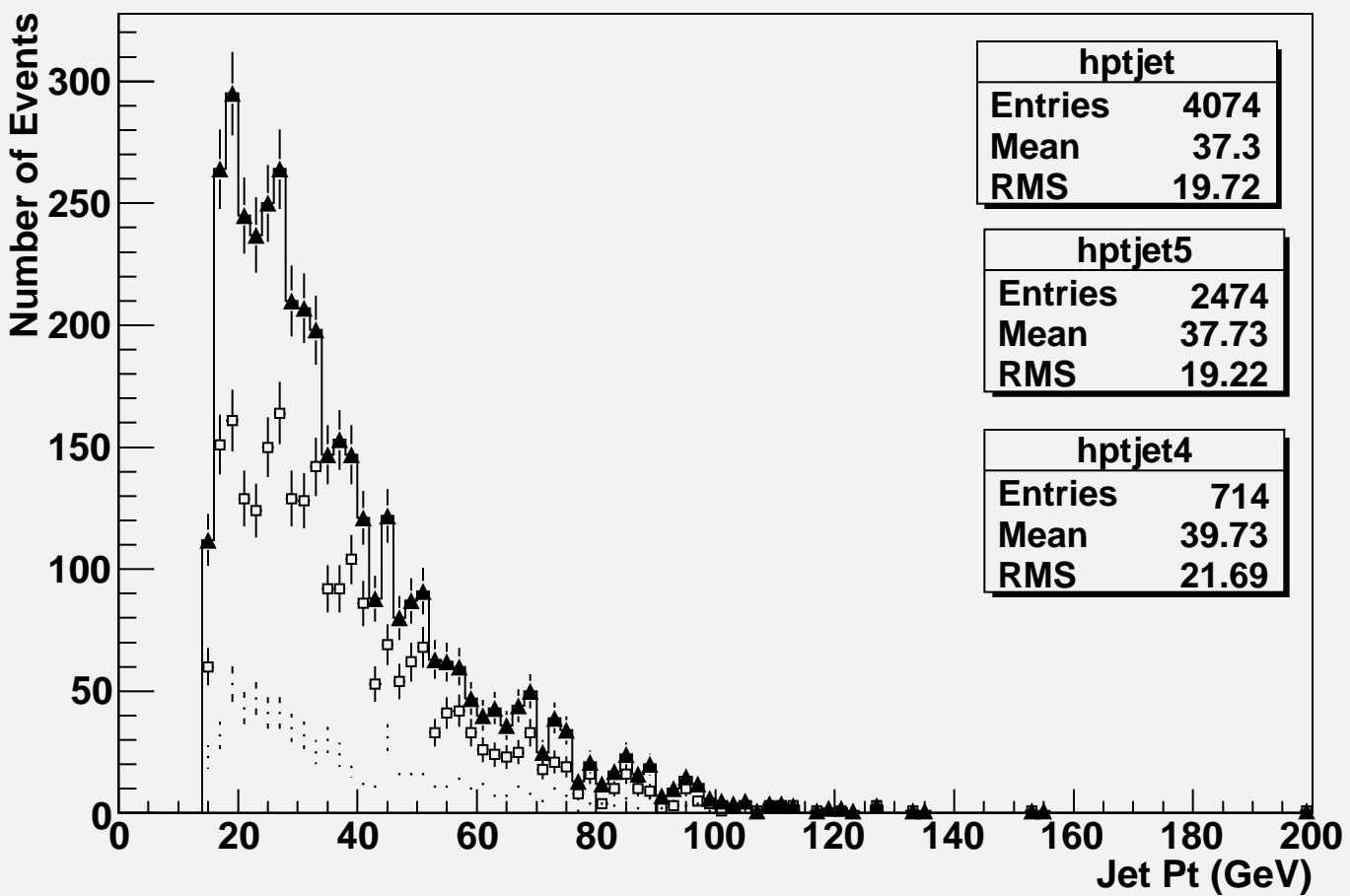
Jet Pt Distribution



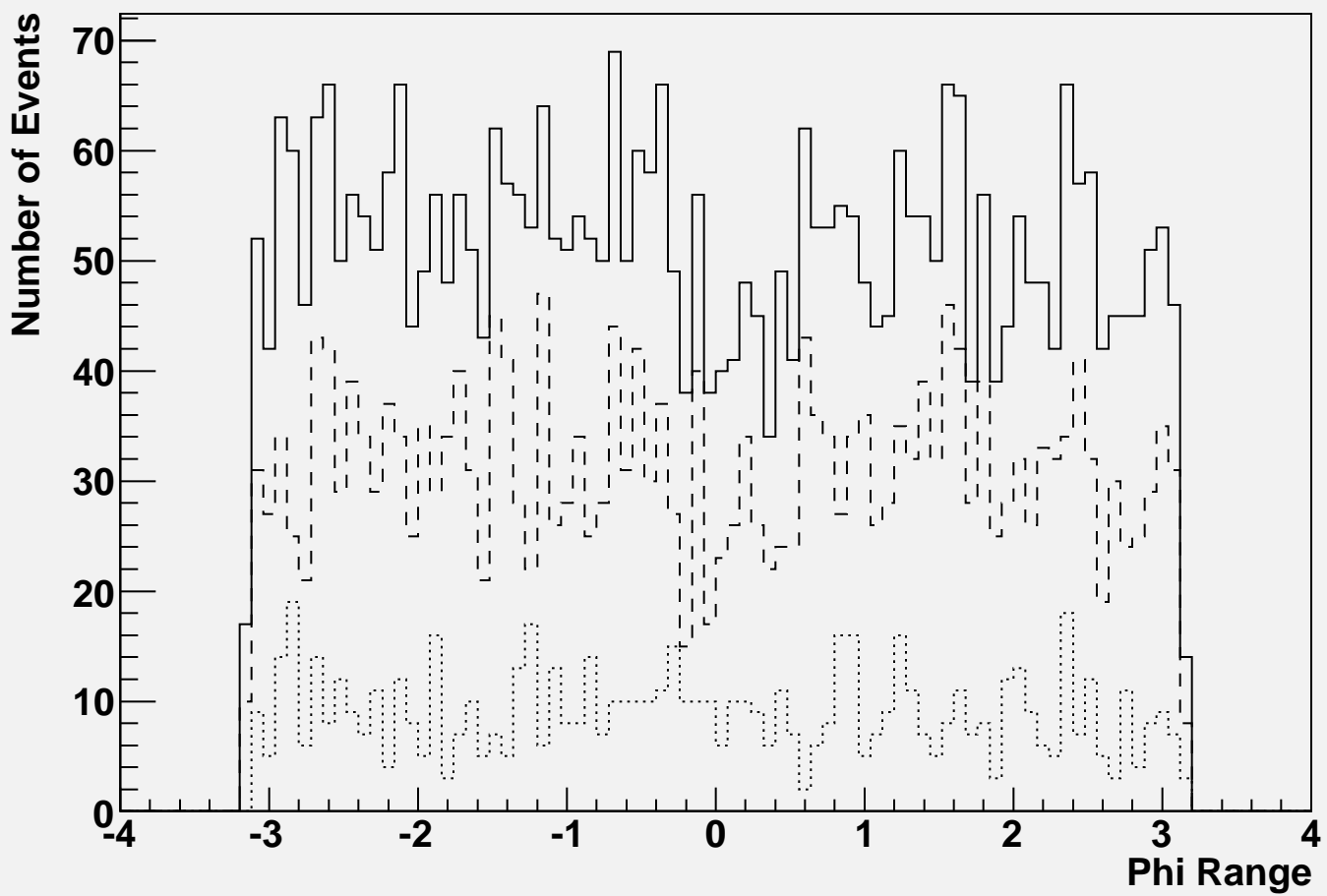
Eta Distribution of the Reconstructed Jets

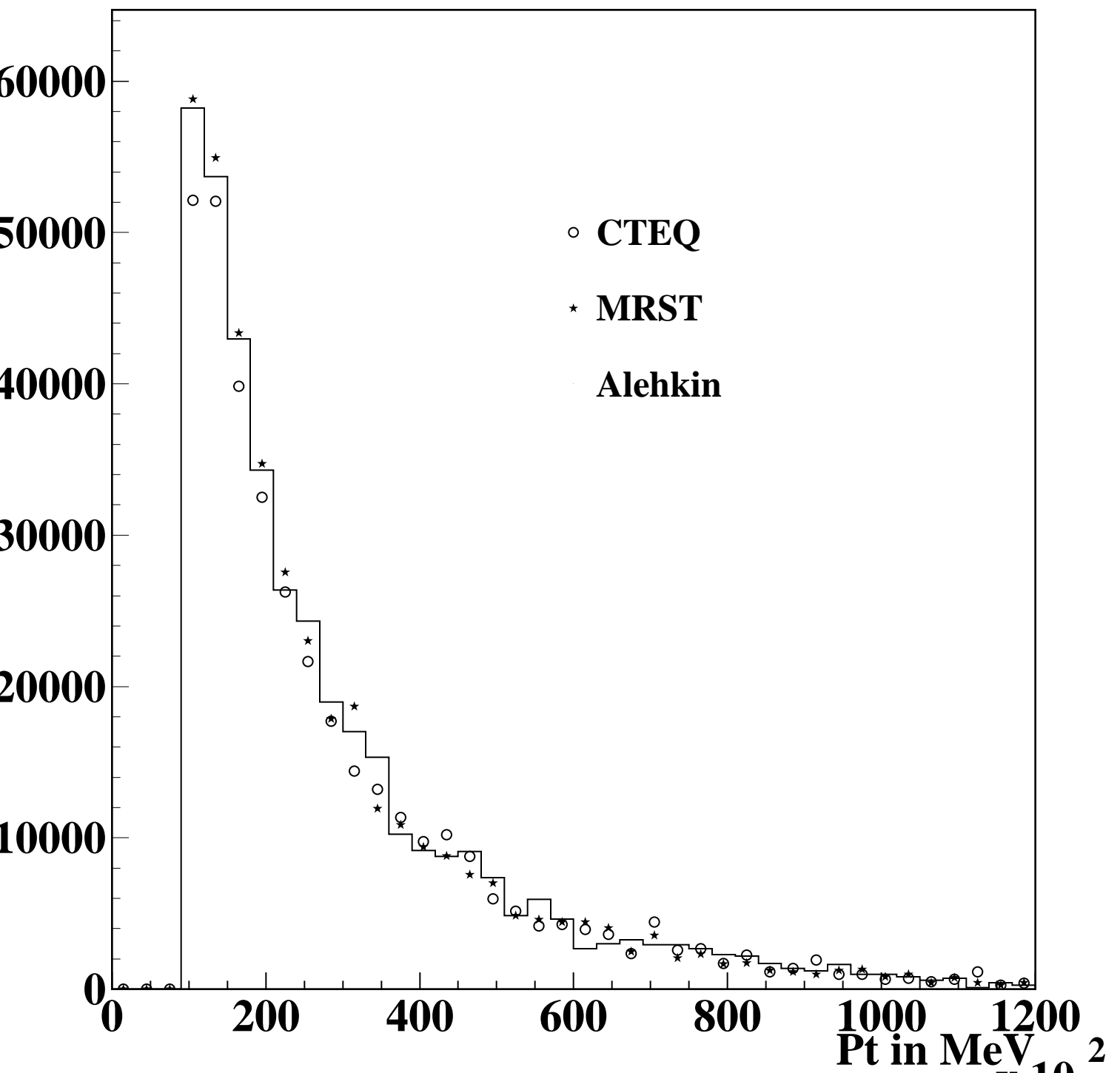


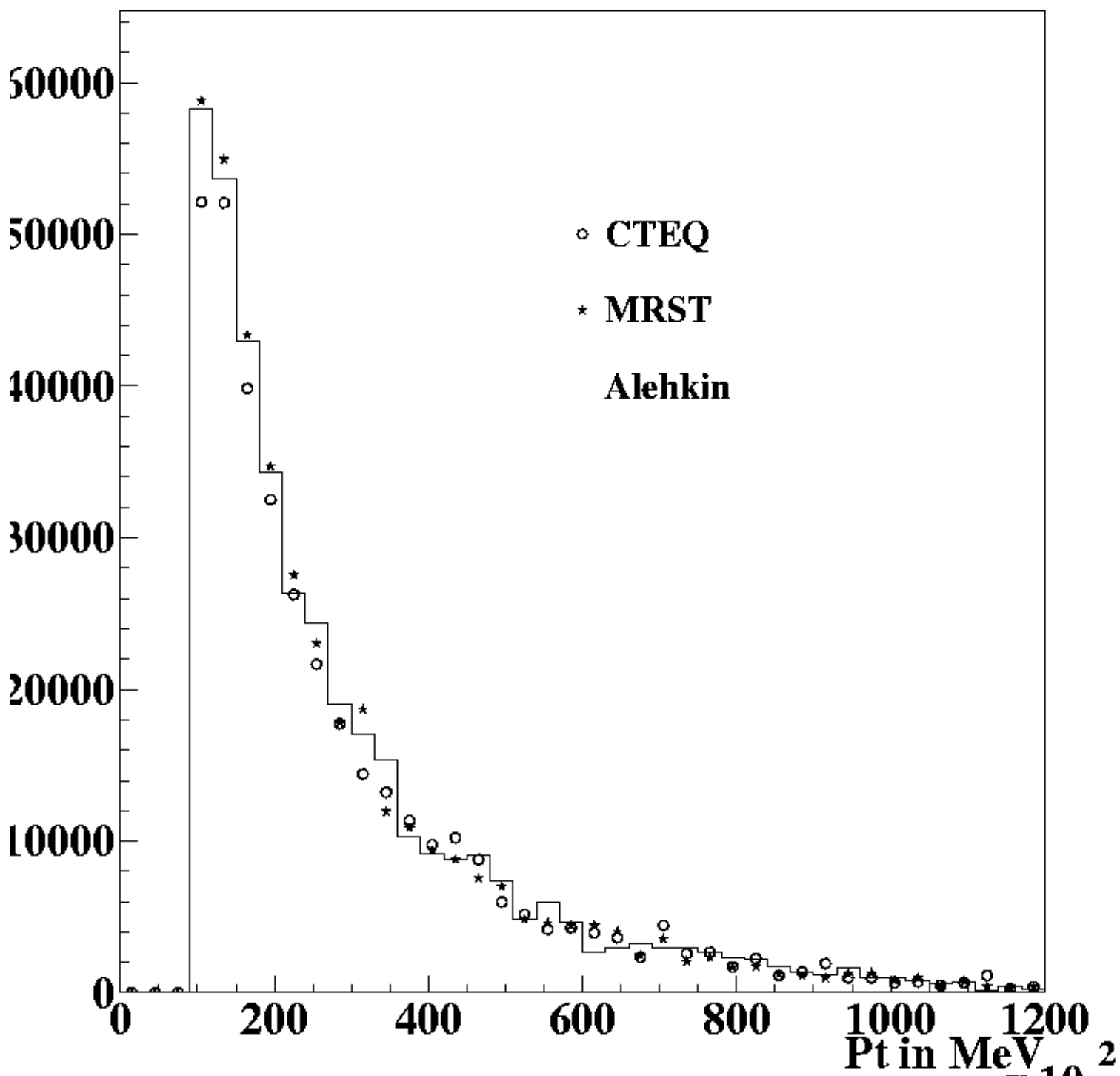
Jet Pt Distribution

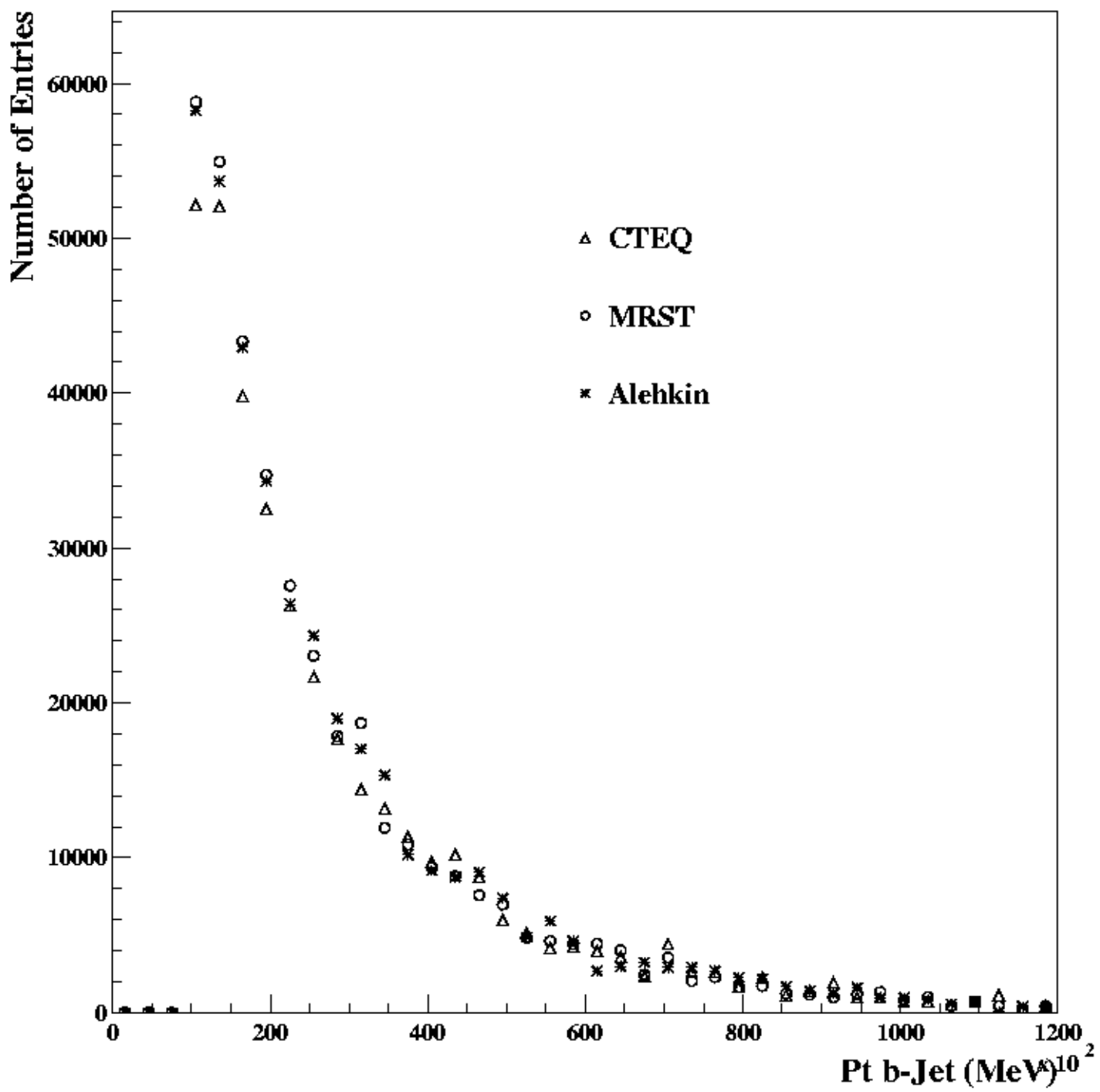


Phi Distribution of Reconstructed Jets

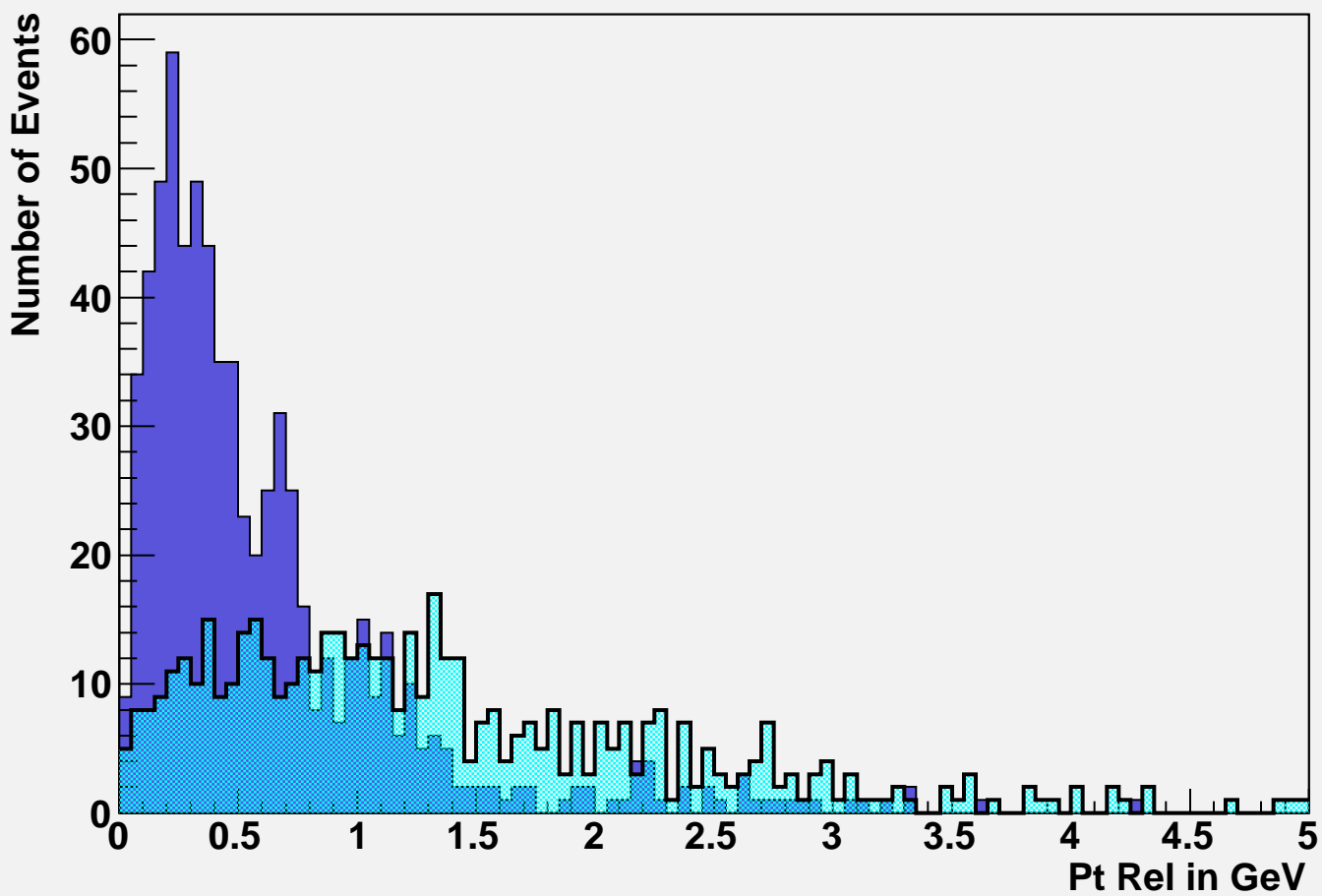




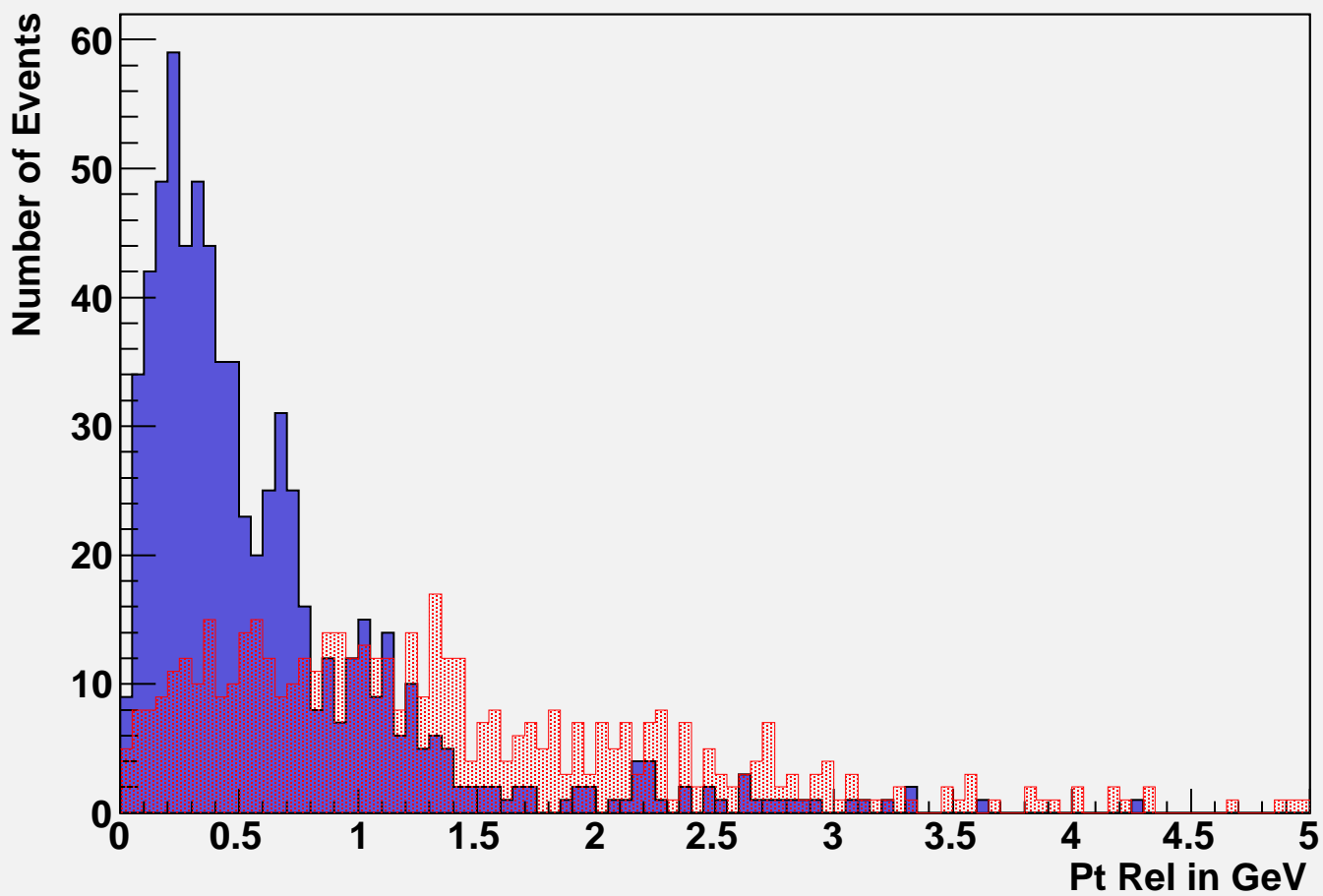


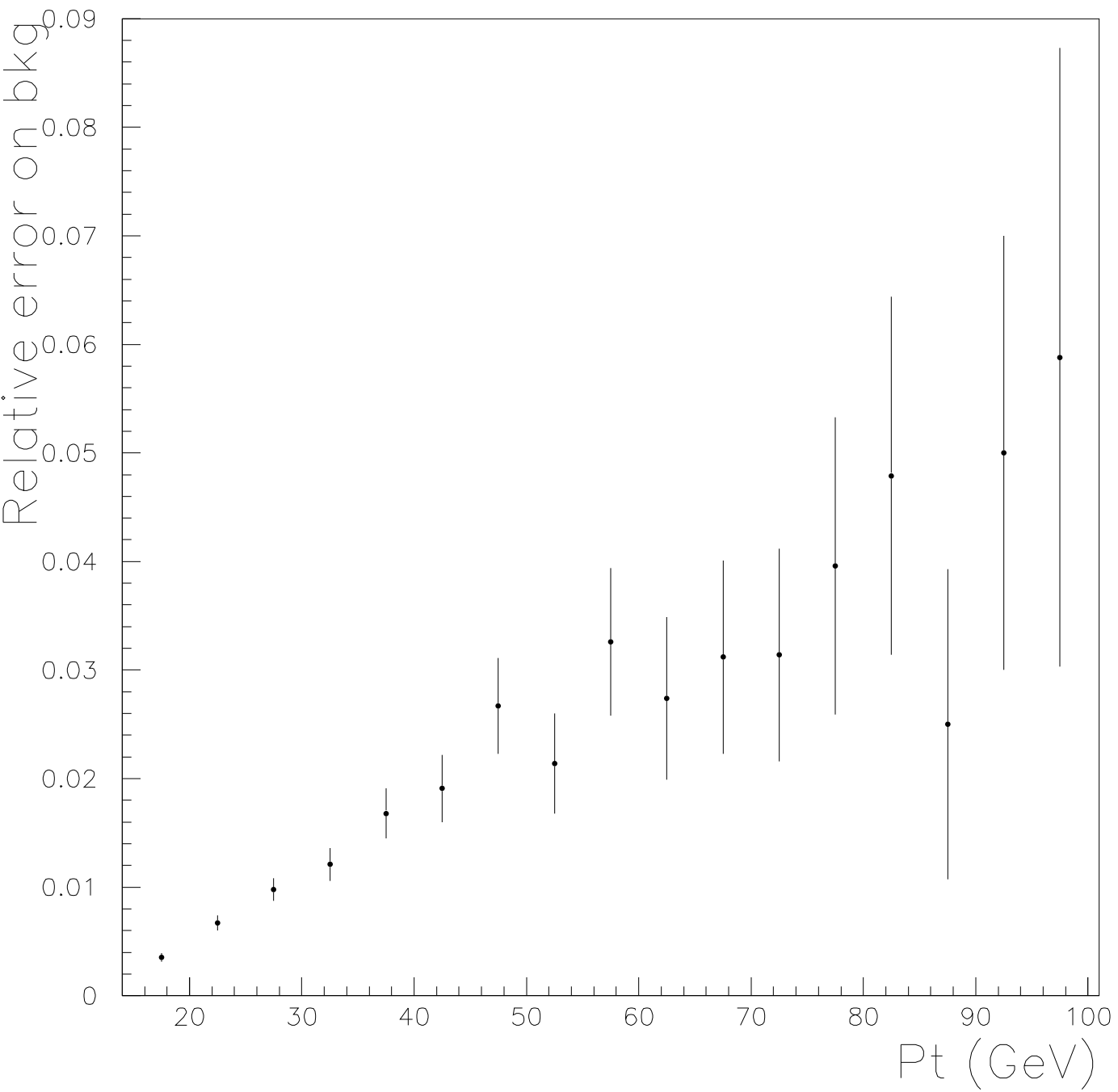


Pt Rel of muon wrt jet



Pt Rel of muon wrt jet





Pt Rel jet-muon

